Success of digital adiabatic simulation with large Trotter step

Changhao Yi

Success of Digital Adiabatic Simulation with Large Trotter Step

Changhao Yi[1, *]

[1]*Center for Quantum Information and Control, University of New Mexico*
(Dated: October 21, 2021)

The simulation of adiabatic evolution has deep connections with Adiabatic Quantum Computation, the Quantum Approximate Optimization Algorithm and adiabatic state preparation. Here we address the error analysis problem in quantum simulation of adiabatic process using Trotter formulas. We show that with additional conditions, the circuit depth can be linear in simulation time T. The improvement comes from the observation that the fidelity error here can't be estimated by the norm distance between evolution operators. This phenomenon is termed as the robustness of discretization in digital adiabatic simulation. It can be explained in three steps, from analytical and numerical evidence: 1. the fidelity error should be estimated by applying adiabatic theorem on the effective Hamiltonian instead. 2. because of the specialty of Riemann-Lebesgue lemma, most adiabatic process is naturally robust against discretization. 3. as the Trotter step gets larger, the spectral gap of effective Hamiltonian tends to close, which results in the failure of digital adiabatic simulation.

I. INTRODUCTION

As one of the most promising applications of quantum computer, the simulation of many body systems [1] has attracted lots of attention in this community. Plenty of novel and efficient methods [2–6] have been studied and implemented over the last few decades. Among them, Trotterization method [7] is a simple and practical one. The basic idea is to separate unitary operator U into small steps, then arrange local gates to approximate each short time evolution. The generated quantum circuits will be a digital evolution operator U_{digital}. A proper estimation of $\|U - U_{\text{digital}}\|$ is necessary to upper bound the gate complexity, for a general initial state, where $\|\cdot\|$ represents the largest singular value of a matrix.

Although the study of the norm distance error $\|U - U_{\text{digital}}\|$ is very mature [8–10], recently, plenty of examples that exhibits the success of Trotterization with large Trotter step have been discovered [11–14], while a convincing analytic explanation is still absent. Suppose in a quantum simulation, the digital evolution operator U_{digital} already deviates a lot from the ideal evolution operator $\|U - U_{\text{digital}}\| \approx 1$, while the quantity of interest is still accurate $\mathcal{Q}[U] \approx \mathcal{Q}[U_{\text{digital}}]$, then we say this simulation is "robust" against rough Trotterization. (As a clarification, lots of previous works focus on the robustness of quantum algorithms against physical decoherence [15–17], while the "robust" in our paper is referred to an intrinsic property of the simulation algorithm.) The quantity of interest can be fidelity between states [11], expectation value of observables [12, 13] and hydrodynamic scaling of correlations [14]. In this work, we address the robustness of digital adiabatic simulation (DAS). More specifically, it's the robustness of scaling index $-\partial \log \epsilon / \partial \log T \approx 1$, where ϵ is the fidelity difference between the state evolved under adiabatic evolution and the corresponding state of the final Hamiltonian; T is the total simulation time, which also quantifies how slow the evolution is. Quantum adiabatic theorem [18–20] provides a proper estimation of ϵ, and the inverse dependence of T is one important feature of it.

Inspired by quantum adiabatic theorem, Adiabatic Quantum Computation (AQC) [21–23] and the Quantum Approximate Optimization Algorithm (QAOA) [24, 25] are two heuristic quantum optimization algorithms that have been widely studied in the last few decades. Both algorithms aim to find the ground state of a complicated system by simulating adiabatic evolution on quantum circuits. In Trotter formula simulation of time-dependent Hamiltonians [26], we not only approximate large unitaries operators with local gates, but also replace the continuous time-ordered evolution operator with the time-averaged version. Its error analysis is different from the time-independent case and has some special properties that help to reduce the complexity [27–29]. So far, different schemes for DAS have been proposed [30–33], while less is known about the apparent robustness [11].

The effective Hamiltonian is a promising tool to explain it. The idea is simple, each Trotterized evolution operator is an exact evolution of effective Hamiltonian. As to DAS, by regarding the digital adiabatic evolution operator as an adiabatic process under effective Hamiltonian, we can apply adiabatic theorem on the effective adiabatic path to obtain an upper bound for digital error. To complete the argument, we further prove that a large class of adiabatic evolution operators is robust against discretization (not Trotterization). The proof is based on a novel discrete form of the Riemann-Lebesgue lemma, which in its continuous formulation is well-known as the principle behind adiabatic theorem. We find that most functions that meet the description of the lemma is robust. However, as the Trotter step gets larger, eventually the robustness fails. Numerical evidence based on gapped systems indicates that this occurs precisely when the effective Hamiltonian becomes gapless along the adiabatic path.

* yichanghao123@unm.edu

The paper is organized as follows. In Sec. II we begin with preliminaries about simulating adiabatic process on quantum circuits, together with previous works about effective Hamiltonian method. In Sec. III we calculate the linear expansion of adiabatic error, and then relate the 1st order term to Riemann-Lebesgue lemma and analyze the robustness of it in Sec. IV. Another important question is why and when this robustness fails, and we attribute it to the shrinking of the effective Hamiltonian spectral gap based on numerical evidence in Sec. V. Finally, in Sec. VI we conclude with discussions about this work and future directions.

II. PREVIOUS WORKS

In this section, we elaborate on the preliminaries about digital adiabatic simulation, then we demonstrate how the argument of effective Hamiltonian can help to provide a better upper bound of fidelity error, and how it efficiently describes the interplay between the adiabatic process and Trotterization procedure.

Given a slow-evolving time-independent Hamiltonian: $\hat{H}(t) = (1-t/T) \cdot H_i + t/T \cdot H_f$ [34] with the initial state $|\psi_i\rangle$ set as one of the ground state of H_i, the evolution operator of the entire process $t \in [0, T]$ is:

$$A := \exp_{\mathcal{T}}\left(-i \int_0^T \hat{H}(t)dt\right) \quad (1)$$

Here we set $\hbar = 1$. If the spectral gap of $\hat{H}(t)$ doesn't close during evolution $t \in [0, T]$ and the evolution is slow enough, then the adiabatic theorem asssures that:

$$\lim_{T \to \infty} A|\psi_i\rangle = |\psi_f\rangle$$

$|\psi_f\rangle$ is the ground state of H_f. We introduce a dimensionless variable $s := t/T$ to simplify the expression:

$$H(s) := \hat{H}(sT), \quad A = \exp_{\mathcal{T}}\left(-iT \int_0^1 H(s)ds\right) \quad (2)$$

Then the fidelity error between $A|\psi_i\rangle$ and $|\psi_f\rangle$ can be quantified by [18]:

$$\sqrt{1 - |\langle\psi_f|A|\psi_i\rangle|^2} \leq \frac{\|H'(0)\|}{T\lambda^2(0)} + \frac{\|H'(1)\|}{T\lambda^2(1)} + \frac{1}{T}\left(\int_0^1 \frac{7\|H'(s)\|^2}{\lambda^3(s)} + \frac{\|H''(s)\|}{\lambda^2(s)}ds\right) \quad (3)$$

where $\lambda(s)$ is the spectral gap of $H(s)$. We denote this complicated upper bound (the RHS) as $\mathcal{G}(T, H)$. The inverse dependence of T and $\lambda(s)$ is the most important feature of the adiabatic theorem.

In AQC, the initial Hamiltonian H_i has a ground state $|\psi_i\rangle$ which is easy to prepare, while H_f has the ground state $|\psi_f\rangle$ encodes the answer we want, or the state we wish to prepare. If we can prepare $|\psi_i\rangle$ and construct A
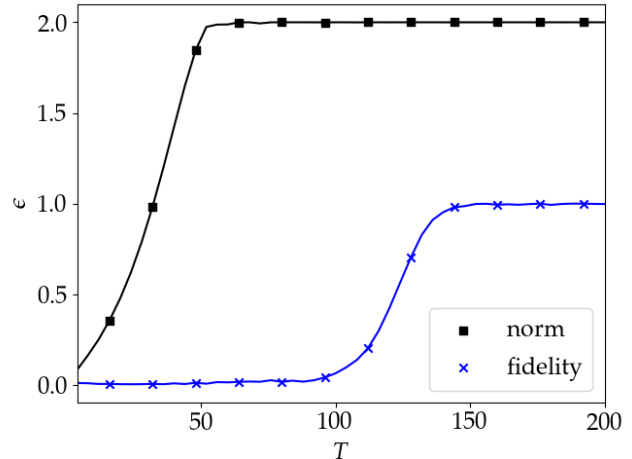

Figure 1. Comparison between norm distance error $\|A_d - A_{\text{tro}}\|$ and fidelity error $\sqrt{1 - |\langle\psi_i|A_d^\dagger A_{\text{tro}}|\psi_i\rangle|^2}$. The Hamiltonian we use throughout this paper is transverse field Ising model $H(s) = (1-s)H_X + sH_Z$ on $N = 8$ sites. $H_X = -\sum_{j=1}^N X_j$, $H_Z = -\sum_{j=1}^N (Z_j + 0.5Z_jZ_{j+1})$ without periodic boundary conditions. In Trotter formula, $H(s)$ is decomposed into $(1-s)H_X$ and sH_Z. L is fixed to 100 while T ranges between [4, 200]. The figure demonstrates that, even when the norm distance error is huge, the fidelity error still remains small. This is an example of robustness of quantum simulation.

faithfully, it will be equivalent to preparing the ground state of H_f. Thus, the central task is to perform the above process on quantum circuits. A common choice for quantum simulation is the first-order Trotter formula $U(\delta t) \approx \prod_k e^{-iH_k\delta t}$. Using this method, the ideal adiabatic operator A is simulated by A_{tro} defined as:

$$A_{\text{tro}} := \prod_{j=1}^L (U_{\text{tro}})_j := \prod_{j=1}^L \prod_{k=1}^\Lambda \exp[-iH_k(s_j)\delta t]$$

where $s_j := (j+1)/L$, L represents the circuit depth, $\delta t := T/L$ is the Trotter step, and the index $k = 1, .., \Lambda$ ranges over the layers in the Hamiltonian (e.g. $H_1 = H_i, H_2 = H_f$). The Trotter error is estimated by [26, 30]:

$$\|A - A_{\text{tro}}\| = \mathcal{O}(\max_{s,k}\|H_k(s)\|^2 T^2/L) \quad (4)$$

To determine the proper choice of T, L, the error we are interested is:

$$\epsilon_{\text{tot}} := \sqrt{1 - |\langle\psi_f|A_{\text{tro}}|\psi_i\rangle|^2} \quad (5)$$

The total error ϵ_{tot} is the actual numerical error on the quantum circuits. It is closely related to:

$$\epsilon_{\text{tro}} := \sqrt{1 - |\langle\psi_i|A_{\text{tro}}^\dagger A|\psi_i\rangle|^2} \quad (6)$$

$$\epsilon_{\text{adb}} := \sqrt{1 - |\langle\psi_f|A|\psi_i\rangle|^2} \quad (7)$$

These three errors satisfies triangular inequality: $\epsilon_{\text{tot}} \leq \epsilon_{\text{adb}} + \epsilon_{\text{tro}}$. ϵ_{adb} is estimated by adiabatic theorem, ϵ_{tro} is upper bounded by the norm distance error in Eq. (4). Therefore, it's natural to conclude that:

$$\epsilon_{\text{tot}} = \mathcal{O}\left(\mathcal{G}(T, H)\right) + \mathcal{O}\left(\max_{s,k} \|H_k(s)\|^2 \frac{T^2}{L}\right)$$

From the above analysis, we can surmise that in DAS there exists the trade-off between two errors: the first one comes from the adiabatic process itself, the second originates in the Trotterization procedure. For fixed L, when T is small, ϵ_{adb} dominates thus ϵ_{tot} is also inversely dependent of T; when T is large, ϵ_{tro} dominates and ϵ_{tot} also starts to increase with T.

However, the norm distance $\|A - A_{\text{tro}}\|$ overestimates the true digital error, for fidelity error ϵ_{tro} and norm distance error can have different error scaling behaviors, and in AQC, only fidelity error matters (whereas the norm error is sensitive to a global phase). In our numerical tests (See Fig. 1), we approximate the ideal adiabatic operator A with the discretized but not Trotterized version A_d:

$$A_d := \prod_{j=1}^{L} U_j, \quad U_j := \exp[-iH(s_j)\delta t] \quad (8)$$

and then compare norm distance error $\|A_d - A_{\text{tro}}\|$ with fidelity error ϵ_{tro}. It's clear that as δt gets larger, the norm distance error quickly increases, while the fidelity error remains small. This difference originates from the specialty of initial state. For example, in the quantum simulation of time-dependent Hamiltonian, when the initial state is an eigenstate, the fidelity error has an upper bound irrelevant to the simulation time [11], while the norm distance error always increases with t.

To exploit the fact that the initial state in DAS is an eigenstate of H_i, a new insight from [11] is to consider the Trotterized evolution operators $(U_{\text{tro}})_j$ as an exact evolution operator of an effective Hamiltonian $\widetilde{H}(s, \delta t)$, then regard A_{tro} as an exact adiabatic process.

$$\widetilde{H}(s, \delta t) := i \log(U_{\text{tro}}(s, \delta t))/\delta t$$

$$A_{\text{tro}} = \prod_{j=1}^{L} \exp[-i\widetilde{H}(s_j, \delta t)\delta t]$$

$$A_{\text{tro}}|\psi_i\rangle \approx \exp_{\mathcal{T}}\left[-iT \int_0^1 \widetilde{H}(s, \delta t)ds\right]|\psi_i\rangle$$

This adiabatic evolution should be able to transform the ground state of $\widetilde{H}(0, \delta t)$ to that of $\widetilde{H}(1, \delta t)$. Under this framework, if $\widetilde{H}(s, \delta t)$ further satisfies:

$$\widetilde{H}(0, \delta t) = H_i \quad , \quad \widetilde{H}(1, \delta t) = H_f$$

Then we can apply adiabatic theorem to effective Hamiltonian as an estimation of the digital error:

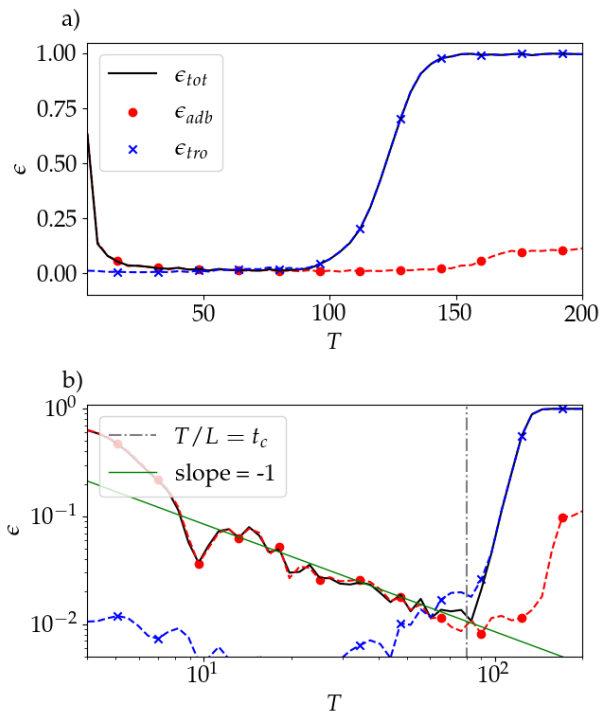$$\epsilon_{\text{tot}} = \mathcal{O}\left(\mathcal{G}(T, \widetilde{H}(s, \delta t))\right) \quad (9)$$

Figure 2. a) The error scaling of three types of errors: ϵ_{adb}, ϵ_{tro} and ϵ_{tot}. The parameters are the same as those in Fig. 1. We use A_d to obtain ϵ_{adb}, thus the simulation fails for large T/L as well. As indicated by the figures, the three types of errors roughly satisfy a linear relation: $\epsilon_{\text{tot}} \approx \epsilon_{\text{adb}} + \epsilon_{\text{tro}}$, which indicates that the total error is determined by the interplay of the adiabatic process and the Trotter splitting. b) The log-log version of the first figure. The scaling index $-\partial \log \epsilon_{\text{tot}}/\partial \log T$ of DAS is robust until $\delta t = t_c \approx 0.8$. In region $T \in [4, Lt_c]$, both errors $\epsilon_{\text{tro}}, \epsilon_{\text{adb}}$ follows the prediction of adiabatic theorem $\epsilon = \mathcal{O}(T^{-1})$. While after the critical point, ϵ_{tro} increases quickly together with ϵ_{tro} for $T \in [Lt_c, 200]$. We say ϵ_{tot} is dominated by ϵ_{adb} in the first region, and dominated by ϵ_{tro} in the second one.

In general cases, even if the above boundary condition is not satisfied, we can still quantify the distance from the ground states of $\widetilde{H}(0, \delta t)$ and $\widetilde{H}(1, \delta t)$ to $|\psi_i\rangle$ and $|\psi_f\rangle$. Then the total error can also be bounded.

This interpretation of digital error is guided by numerical tests. Fig. 2 illustrates the error scaling of ϵ_{tot} with respect to T for fixed L. When δt is small, $\widetilde{H}(s, \delta t)$ is very similarly to the original Hamiltonian $H = \widetilde{H}(s, 0)$, therefore $\epsilon_{\text{tro}} \approx \epsilon_{\text{adb}}$ and the overall scaling of $\mathcal{O}(T^{-1})$ is the same with the non-Trotterized version; when δt gets larger, the discrete adiabatic process itself gets more "coarse", and the perturbation to the original adiabatic path $\widetilde{H}(s, \delta t) - H(s)$ gets larger. We believe in our simulation the perturbation causes the closure of spectral gap, thus the adiabatic evolution won't give us the right final state, the error increases accordingly. In the following sections, we intend to rigorize the above observations with analytic and numerical results.

III. EXPANSION OF ADIABATIC ERROR

The previous analysis [11] assumed the discretization error was negligible in order to focus on the effect of Trotterization. Here we establish the region for the estimation of ϵ_{tot} in Eq. (9) to be valid. Based on the effective Hamiltonian method, the analysis of ϵ_{tro} essentially boils down to the adiabatic error of A_d for general adiabatic path $H(s)$. In this section, we begin with the study of the linear expansion of adiabatic error ϵ_{adb} for the discrete adiabatic operator A_d. Similar questions have been studied in [19, 35, 36], while here we use a different approach to derive it. We also require $H(s)$ to be non-degenerate : $\forall l \neq m, E_l(s) \neq E_m(s)$.

Follow the definition in Eq. (8), each evolution operator U_j can be diagonalized as:

$$U_j = B_j \hat{\Lambda}_j B_j^{\dagger}$$

where B_j encodes the eigenbasis of H_j, $(\hat{\Lambda}_j)_{ll} = \exp[-iE_l(j)\delta t]$. Here l labels the energy level, and j labels the index of time step. In adiabatic analysis, a common trick is to replace $H(s)$ with $H(s) - E_0(s)$, as the effect of this transformation is merely an extra phase in A_d. After this simplification procedure, the new diagonal matrix Λ_j can be written as:

$$(\Lambda_j)_{ll} = e^{-i\lambda_l(j)\delta t}, \quad \lambda_l(j) := E_l(j) - E_0(j)$$

In the product of evolution operators U_j, we merge the neighboring eigenbasis matrices into a transition matrix:

$$S_j := B_{j+1}^{\dagger} B_j, \quad (S_j)_{lm} = \langle l(j+1)|m(j)\rangle$$

where $|m(j)\rangle$ denotes the m-th eigenstate of Hamiltonian $H(s_j)$. With the new notations, we obtain:

$$A_d = B_L \Gamma B_1^{\dagger}, \quad \Gamma := \Lambda_L \prod_{j=1}^{L-1} S_j \Lambda_j$$

Since:

$$B_1^{\dagger}|\psi_i\rangle = B_L^{\dagger}|\psi_f\rangle = (1, 0, \cdots, 0)^T$$

The adiabatic error is directly related to Γ:

$$\epsilon_{\mathrm{adb}} = \sqrt{1 - |\langle \psi_f | A_d | \psi_i\rangle|^2} = \sqrt{1 - \Gamma_{00}}$$

And Γ matrix can be illustrated as:

$$\Gamma = \begin{pmatrix} \sqrt{1-\epsilon_{\mathrm{adb}}^2} & \cdot & \cdot & \cdot \\ \bar{\epsilon}_1 & \cdot & \cdot & \cdot \\ \bar{\epsilon}_2 & \cdot & \cdot & \cdot \\ \cdot & \cdot & \cdot & \cdot \end{pmatrix} \quad (10)$$

$\bar{\epsilon}_l$ is the undesired transition amplitude to the l-th energy level of the final Hamiltonian. The linear expansion of $\{\bar{\epsilon}_l\}$ can be derived from the linear expansion of Γ. Notice that δt is not regarded as a tiny quantity here, while $\{S_j\}$

are all close to identity. Therefore, Γ can be expanded in terms of the off-diagonal parts of $\{S_j\}$:

$$\Gamma = \Gamma^{(0)} + \Gamma^{(1)} + \cdots$$
$$= \prod_{j=1}^{L} \Lambda_j + \sum_{k=1}^{L} \left(\prod_{j>k} \Lambda_j\right)(S_k - I)\left(\prod_{j<k} \Lambda_j\right) + \cdots$$

$\Gamma^{(q)}$ is equivalent to the summation of q-th jump paths in [35]. The leading term $\Gamma^{(0)}$ doesn't contribute to $\{\bar{\epsilon}_l\}$. Thus, we approximate $\bar{\epsilon}_l$ with the off-diagonal elements of $\Gamma^{(1)}$, and obtain:

$$\epsilon_l := \frac{1}{L}\sum_{k=1}^{L-1} \theta_l(k) \exp\left[-i\frac{T}{L}\sum_{j<k}\lambda_l(j)\right] \quad (11)$$

with:

$$\theta_l(j) := \langle l'(j)|0(j)\rangle = \frac{\langle l(j)|H'(s_j)|0(j)\rangle}{\lambda_l(j)} \quad (12)$$

The adiabatic error is the summation of undesired transition probabilities:

$$\epsilon_{\mathrm{adb}}^2 \approx \sum_{l>0} |\epsilon_l|^2 \quad (13)$$

The expression of ϵ_l is close to the function described by Riemann-Lebesgue lemma [19]. To see this, consider the continuous limit $L \to \infty$:

$$\lim_{L\to\infty} \epsilon_l = \int_0^1 \theta_l(s) \exp\left[-iT \int_0^s \lambda_l(s')ds'\right] ds$$
$$= \int_{\Omega_l(0)}^{\Omega_l(1)} \frac{\theta_l(\Omega_l^{-1}(y))}{\lambda_l(\Omega_l^{-1}(y))} e^{-iTy} dy \quad (14)$$

where $\Omega_l(s) := \int_0^s \lambda_l(s')ds'$.

As a brief analysis, $\theta_l(s)$ itself is proportional to $\|H'(s)\|/\lambda_l$, there's another factor of $1/\lambda_l$ comes from changes of variable in Eq. (14). Therefore, the first term in the expansion of the adiabatic error ϵ_{adb} has order $\mathcal{O}(\|H'\|/T\lambda_1^2)$, which matches with the prediction of the adiabatic theorem.

To simplify the question, we focus on the case where $\sum_{l>0} |\epsilon_l|^2$ is the only term in $\epsilon_{\mathrm{adb}}^2$ with order $\mathcal{O}(T^{-2})$. This estimation is not complete in general, as an instance, the famous Marzlin-Sanders counterexample [20] can't be explained in this way. The issue is not about $\{\epsilon_l\}$, it's because sometimes $\Gamma^{(1)}$ is not enough to approximate Γ. Fortunately, the higher order expansions of Γ and the continuous limit have been systematically studied. Researchers proved that (See Corollary 1 in [35]), if $\|H''(s)\| = o(\sqrt{T})$, $\|H'''(s)\| = o(T)$ and $\|H'(s)\|, (\min_{l,m}|E_l - E_m|)^{-1}$ have constant upper bounds, then $\sum_{l>0} \epsilon_l|l(1)\rangle$ is the leading term of $(1 - |\psi_f\rangle\langle\psi_f|)A|\psi_i\rangle$ with proper choice of phase. Therefore, under this premise, we can focus on the behavior of $\{\epsilon_l\}$ under discretization.

IV. ROBUSTNESS OF DISCRETE RIEMANN-LEBESGUE LEMMA

In Sec. III we proved that, the leading term of the undesired transition rate to higher energy levels of H_f is a discrete sum version of integrals in the form:

$$I = \int_0^1 f(s) \exp[-iTg(s)]ds, \quad g'(s) > 0 \qquad (15)$$

Using Riemann-Lebesgue lemma, it's immediate to see the amplitude of the above integral has order $\mathcal{O}(T^{-1})$. In our situation, the question of interest is how robust the scaling is with respect to discretization. Usually, an integral is calculated numerically in this method:

$$\int_a^b c(s)ds \to \sum_{k=1}^{L} \frac{1}{L}c(s_k), \quad s_k = a + (b-a)\frac{k}{L}$$

The error has order $\mathcal{O}(|c'(s)|/L)$. In Eq. (15), the derivative of integrand has order $\mathcal{O}(T)$, while we don't necessarily need L to be much larger than T to obtain the overall scaling of $\mathcal{O}(T^{-1})$. A simple example is the case where $f(s) = 1, g(s) = s$, both the discrete version and the exact value of the integral can be solved analytically:

$$I' = \int_0^1 e^{-iTs}ds = \frac{1}{iT}[1 - e^{-iT}]$$

$$I'_d = \frac{1}{L}\sum_{k=1}^{L} e^{-ikT/L} = e^{-iT/L}\frac{1 - e^{-iT}}{L(1 - e^{-iT/L})}$$

Compare their amplitudes, we find that as long as $0 < T/L < 3.78$, the difference between $|I'|$ and $|I'_d|$ is merely a factor of 2. While in error analysis, we only care about the parameter dependence of T, this factor of 2 can totally be ignored. On the other hand, when $T/L = 2\pi$, $|I'_d| = 1$ is much larger than $|I'| = O(T^{-1})$, thus the simulation fails. Essentially this is the reason why the discretization error is negligible in DAS even for large δt, and the simulation breaks down as δt continues to grow.

The above reasoning can be generalized to the following theorem, which is one of our main results (See Appendix A):

Theorem 1 (Discrete Riemann-Lebesgue lemma). $f(s)$ is a L^1 integrable, second-differentiable complex function defined on $[0, 1]$, $\lambda(s)$ is a first-differentiable positive real function. Denote $f(s_k), s_k \in [0, 1]$ as f_k, then consider the following discrete summation:

$$J := \frac{1}{L}\sum_{k=1}^{L} f_k \exp\left[-i\frac{T}{L}\sum_{j<k}\lambda_j\right]$$

Defining $\delta t := T/L$. If $\max_s \lambda(s)\delta t < 3.78$, we have:

$$|J| = \mathcal{O}\left(\frac{1}{T}\max_{s=0,1}\frac{|f(s)|}{\lambda(s)} + \frac{1}{T^2}\max_{s=0,1}\frac{|\eta(s)|}{\lambda(s)}\right) + \mathcal{O}\left(\frac{\mathcal{A}(\eta, \lambda)}{T^2}\right)$$
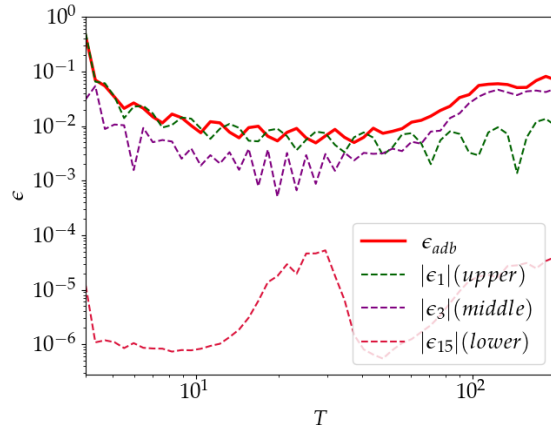

Figure 3. Error scaling of $|\epsilon_1|$ (the upper dahsed line), $|\epsilon_3|$ (the middle dashed line) and $|\epsilon_{15}|$ (the lower dashed line) in log-log figure. The Hamiltonian here is the same as that of Fig. 1 with $N = 4$. As predicted by Theorem 1, the scaling $\epsilon_l = \mathcal{O}(T^{-1})$ breaks down when $\max_s \lambda_l \delta t \approx 2\pi$. Thus, although ϵ_{adb} (the solid line) is dominated by $|\epsilon_1|$ at the beginning, its robustness breaks down with $|\epsilon_3|$ for $\lambda_3 > \lambda_1$; $|\epsilon_{15}|$ has larger energy gap, but its overall amplitude is too small to influence ϵ_{adb}.

where:

$$\eta(s) := L\left(\frac{f(s)}{\omega(s)} - \frac{f(s - 1/L)}{\omega(s - 1/L)}\right) \approx \left(\frac{f(s)}{\omega(s)}\right)'$$

$$\omega(s) := \frac{1}{i\delta t}(e^{-i\delta t\lambda(s)} - 1)$$

and

$$\mathcal{A}(\eta, \lambda) := \int_0^1 \left|\left(\frac{\eta(s)}{\omega(s)}\right)'\right|ds$$

Shortly speaking, Theorem 1 implies that as long as the Hamiltonian is stable in the sense that T is much larger than $|\lambda'_l|, |\theta'_l|$ and $|\theta''_l|$, and $\max \lambda_l(s)\delta t < 3.78$, the leading term of adiabatic error is very close to the continuous limit. To make sure every ϵ_l is robust, it's sufficient to have $\max_{s,l} |E_l(s) - E_0(s)|\delta t < 3.78$. This conclusion is a little counterintuitive: although the value of ϵ_{adb} is determined by the smallest spectral gap, its robustness is controlled by the largest spectral gap. Also, in practice, the amplitude of ϵ_m with high energy level λ_m can be too small to influence ϵ_{adb}, which makes A_d more robust than predicted. (See Fig. 3)

Follow Theorem 1, we obtain the discrete analogue of Corollary 1 in [35] (See Appendix B):

Corollary 1 (Robustness of discrete adiabatic process). *Given the discrete adiabatic operator defined in Eq. (8), if:*

$$\|H'\| = \mathcal{O}(1), \quad \|H''\| = o(\sqrt{T}), \quad \|H'''\| = o(T) \quad (16)$$

$$(\min_{l,m,s} |E_l(s) - E_m(s)|)^{-1} = \mathcal{O}(1) \qquad (17)$$

and $\max_{l,s} \lambda_l(s)\delta t < 3.78$, then:

$$\epsilon_{adb} = \mathcal{O}\left(\max_{s=0,1} \frac{\|H'(s)\|}{T\lambda_1^2(s)}\right)$$

V. A NUMERICAL TEST FOR THE CLOSURE OF ENERGY GAP

In previous sections, we prove that when the Trotter step remains in certain region $\delta t = \mathcal{O}(1/\max_{l,m,s} |E_l(s) - E_m(s)|)$, and $H(s)$ doesn't have a fast driven oscillation term, then the prediction of adiabatic theorem is accurate $\epsilon = \mathcal{O}(T^{-1})$. However, the sharp increase of total error (See Fig. 2) at a threshold value t_c requires extra explanation. There are several reasons that might account for the instability of DAS : the effective adiabatic path $\widetilde{H}(s, \delta t)$ itself might differ substantially from $H(s)$, or the discretization procedure may no longer be robust. In this section we demonstrate that, in the model we use (See Fig. 1), the threshold phenomenon coincides with the closure of the spectral gap in $\widetilde{H}(s, \delta t), s \in [0, 1]$.

The rigorous calculation of $\widetilde{H}(s, \delta t)$ is easy when δt is less than $\mathcal{O}(\lambda/N)$ [11], while the same expression is hard to analyze both analytically and numerically for large δt. The issue is in determining the correspondence of the eigenstates of $U_{\mathrm{tro}}(\delta t)$ and those of $H(s)$ when δt is $\Omega(1)$. To overcome this we propose a numerical test that detects the closing of the spectral gap around the eigenstate of interest without resorting to calculating the energy levels of $\widetilde{H}(s, \delta t)$. The intuition originates from the quantum Zeno effect [31, 37]. Given an adiabatic path $\{H(s_j)\}$, at each step we project current ground state $|\psi_j\rangle$ to that of the next Hamiltonian $|\psi_{j+1}\rangle$, then eventually, we obtain a state very close to the ground state of $H(1)$.

$$H(s_0) \to H(s_1) \to \cdots \to H(s_{L-1})$$
$$|\psi_0\rangle \to |\psi_1\rangle \to \cdots \to |\psi_{L-1}\rangle$$

In the numerical test, we choose the initial state $|\phi_0\rangle$ as the ground state of the first Hamiltonian $H(0)$. We increase the value of s gradually from 0 to 1. At each step $s = s_j$, we calculate the eigenbasis of the next Hamiltonian $H(s_{j+1})$. Among these quantum states, we pick the one with largest overlap with $|\phi_j\rangle$ as our next "ground state" $|\phi_{j+1}\rangle$. The process ends when $s = 1$ and we term it a "test of near degeneracy". If the interval $1/L$ is small enough : $1/2 > \|H'(s_j)\|/L\lambda_j$, the generated states $\{|\phi_j\rangle\}$ should all be ground states of $H(s_j)$. While it's possible that this largest overlap deviates a lot from 1 even when $1/L$ is very small. This indicates a gapless point and can be explained by the perturbation theory of degenerate state.

Suppose $H(s)$ has degenerate ground states $|\alpha\rangle, |\beta\rangle$ at certain point s_*, then in this degenerate subspace Π,
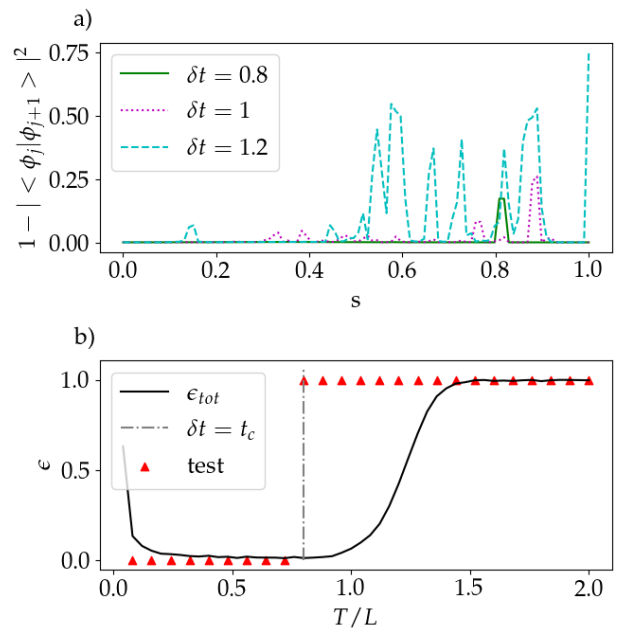
Figure 4. a) Record of the fidelity distance between neighboring "ground states" $1 - |\langle\phi_j|\phi_{j+1}\rangle|^2$ generated from the numerical test with $\delta t = 0.8, 1, 1.2$, which correspond to solid line, dotted line and dashed line separately. For most steps, the overlap $|\langle\phi_j|\phi_{j+1}\rangle|^2$ is very close to 1; at some points the overlap deviates a lot from 1, which implies a closing spectral gap. As δt gets larger, the test gets more and more unstable. b) The black line is the total error of DAS in Fig. 2. For each Trotter step δt, we perform the test of near degeneracy on the effective Hamiltonian $\widetilde{H}(s, \delta t)$ with the ground state of H_X as initial state. If during the test, the largest overlap is larger than 0.99, then we regard the test as success and return 0. Otherwise the test fails, and we return 1. The test demonstrates whether the spectral gap of $\widetilde{H}(s, \delta t)$ closes during $s : 0 \to 1$. As indicated by the figure, the spectral gap closes around $\delta t \approx 0.8$. This matches with the turning point t_c of ϵ_{tot}.

$H(s_*)$ is proportional to identity.

$$H(s_*)\Big|_{\Pi} = E_* \begin{pmatrix} 1 & 0 \\ 0 & 1 \end{pmatrix}$$

Any vector in the degenerate subspace can be an eigenstate of $H(s_*)$. Thus, the numerical result of the eigenstate of $H(s_*)$ with energy E_* can be any state of form $c_\alpha|\alpha\rangle + c_\beta|\beta\rangle$. In the next step $s = s_* + ds$:

$$H(s_* + ds)\Big|_{\Pi} \approx E_* \begin{pmatrix} 1 & 0 \\ 0 & 1 \end{pmatrix} + ds H'(s_*)\Big|_{\Pi}$$

If $H'(s_*)$ doesn't commute with $H(s_*)$ in subspace Π, the eigenstate of $H(s)$ is arbitrary while the eigenstates of $H(s_* + ds)$ is fixed to be that of the perturbation term. As a result, in the test of near degeneracy, the degenerate ground state of $H(s_*)$ won't find an eigenstate of $H(s_* + ds)$ with overlap close to 1 as the algorithm doesn't derive ground states based on the perturbation

of the next step. A similar thing happens if $H(s_*)$ is not degenerate while $H(s_* + ds)$ is, or if there exists degenerate point s^* between neighboring samples $s_1 < s^* < s_2$. We can easily witness this phenomenon (See Fig. 4a), all points that deviates a lot from 1 represent a degenerate subspace.

Although the spectrum of $\widetilde{H}(s, \delta t)$ is calculated indirectly, the eigenbasis of $\widetilde{H}(s, \delta t)$ is the same with that of $U_{\text{tro}}(s, \delta t)$, we can thus use this information to detect whether there exists degenerate ground states during the evolution $s \in [0, 1]$. If we find near degeneracy, then we also know that the spectral gap of $\widetilde{H}(s, \delta t)$ is closing. As indicated by numerical results (See Fig. 4b), the test fails with the robustness of DAS. We witnessed the same phenomenon in other numerical models. These tests support our conjecture that the error increases sharply as the spectral gap of $\widetilde{H}(s, \delta t)$ closes.

VI. CONCLUSION

The robustness of DAS here has two meanings: a very broad class of adiabatic path $H(s)$ is robust against rough discretization, and the effective Hamiltonian $\widetilde{H}(s, \delta t)$ is robust in the sense that $\mathcal{G}(T, \widetilde{H}(s, \delta t)) \approx \mathcal{G}(T, H(s))$ for large δt. If both conditions are satisfied, then the circuit depth of DAS is linear in T. In this work, we focus on the first point and provide strict analysis about it; as to the second point, because of the lack of proper analytic methods, we only provide numerical evidence that supports our explanation. However, in practical implementation of DAS, the second point is the factor that sets restriction on δt. Here we propose several possible solutions to find the critical point t_c where the spectral gap of $\widetilde{H}(s, \delta t)$ vanishes.

The first solution, of course, is to provide a strict analysis of $\widetilde{H}(s, \delta t)$. Certainly, the spectral gap won't close if the perturbation in spectral norm $\|\widetilde{H}(s, \delta t) - H(s)\|$ is smaller than the original spectral gap λ. For a 1d 2-local normalized Hamiltonian supported on N sites, it's equivalent to have $\delta t = \mathcal{O}(\lambda/N)$. However, the estimation is not enough to explain the robustness. This direction doesn't look promising, but some rigorous results of the

Floquet operator [38] might help.

The other approach is to find t_c numerically. Although the numerical test in Sec. V gives us a good estimation of of t_c, it's impractical to perform it on large systems, as exact diagonalization procedure will be too inefficient. The question can be formulated as follows: given a quantum state $|\Psi\rangle$ and a unitary quantum circuit C, how to output the eigenstate of C with largest overlap with $|\Psi\rangle$? Some previous works [39] might shed light on quantum solutions to this problem. Besides, it's not surprising that as δt gets larger, the spectral gap of $\widetilde{H}(s, \delta t)$ will close. The confusing phenomenon in Fig. 4 is, after the critical point $\delta t > t_c$, the spectral gap will always close for some $s_* \in [0, 1]$. The reason might be related to the delocalization property of Floquet operators [12, 13].

There have been many papers working on the connections between QAOA and AQC [40–46], the robustness of DAS might be one of them. We argue that, given fixed H_i and H_f, by properly choosing function $p(s)$, the adiabatic path $H(s) = [1 - p(s)]H_i + p(s)H_f$ can be very robust. Thus, the restriction on "Trotter step" can be very loose. This might be one direction that exhibits the efficiency of QAOA through the framework of AQC. Tools in QAOA, like energetic cost and quantum speed limit, can be applied to study digital adiabatic process as well.

The expansion of adiabatic error itself has some mystery as well. Comparing to another adiabatic theorem [18], we find that the distance between two arbitrary energy levels $|E_l - E_m|$ shouldn't appear in the expression of adiabatic theorem, and there should be two extra terms of order $\mathcal{O}(\|H'\|^2/T\lambda^3)$ and $\mathcal{O}(\|H''\|/T\lambda^2)$. We conjecture that it's possible to find space for improvement in both methods.

VII. ACKNOWLEDGEMENT

[1] Richard P Feynman. Simulating physics with computers. *Int. J. Theor. Phys*, 21(6/7), 1982.

[2] Guang Hao Low and Isaac L Chuang. Hamiltonian simulation by qubitization. *Quantum*, 3:163, 2019.

[3] Andrew M Childs and Nathan Wiebe. Hamiltonian simulation using linear combinations of unitary operations. *arXiv preprint arXiv:1202.5822*, 2012.

[4] Earl Campbell. Random compiler for fast hamiltonian simulation. *Physical review letters*, 123(7):070503, 2019.

[5] Paul K Faehrmann, Mark Steudtner, Richard Kueng, Maria Kieferova, and Jens Eisert. Randomizing multi-product formulas for improved hamiltonian simulation. *arXiv preprint arXiv:2101.07808*, 2021.

[6] Yuan Su, Dominic W Berry, Nathan Wiebe, Nicholas Rubin, and Ryan Babbush. Fault-tolerant quantum simulations of chemistry in first quantization. *arXiv preprint arXiv:2105.12767*, 2021.

[7] Seth Lloyd. Universal quantum simulators. *Science*, pages 1073–1078, 1996.

[8] Andrew M Childs and Yuan Su. Nearly optimal lattice simulation by product formulas. *Physical review letters*, 123(5):050503, 2019.

[9] Andrew M Childs, Yuan Su, Minh C Tran, Nathan Wiebe, and Shuchen Zhu. Theory of trotter error with commutator scaling. *Physical Review X*, 11(1):011020, 2021.

[10] Minh C Tran, Su-Kuan Chu, Yuan Su, Andrew M Childs, and Alexey V Gorshkov. Destructive error interference in product-formula lattice simulation. *Physical review letters*, 124(22):220502, 2020.

[11] Changhao Yi and Elizabeth Crosson. Spectral analysis of product formulas for quantum simulation. *arXiv preprint arXiv:2102.12655*, 2021.

[12] Markus Heyl, Philipp Hauke, and Peter Zoller. Quantum localization bounds trotter errors in digital quantum simulation. *Science advances*, 5(4):eaau8342, 2019.

[13] Lukas M Sieberer, Tobias Olsacher, Andreas Elben, Markus Heyl, Philipp Hauke, Fritz Haake, and Peter Zoller. Digital quantum simulation, trotter errors, and quantum chaos of the kicked top. *npj Quantum Information*, 5(1):1–11, 2019.

[14] Jonas Richter and Arijeet Pal. Simulating hydrodynamics on noisy intermediate-scale quantum devices with random circuits. *Physical Review Letters*, 126(23):230501, 2021.

[15] Andrew M Childs, Edward Farhi, and John Preskill. Robustness of adiabatic quantum computation. *Physical Review A*, 65(1):012322, 2001.

[16] MS Sarandy and DA Lidar. Adiabatic quantum computation in open systems. *Physical review letters*, 95(25):250503, 2005.

[17] Johan Åberg, David Kult, and Erik Sjöqvist. Quantum adiabatic search with decoherence in the instantaneous energy eigenbasis. *Physical Review A*, 72(4):042317, 2005.

[18] Sabine Jansen, Mary-Beth Ruskai, and Ruedi Seiler. Bounds for the adiabatic approximation with applications to quantum computation. *Journal of Mathematical Physics*, 48(10):102111, 2007.

[19] Mohammad HS Amin. Consistency of the adiabatic theorem. *Physical review letters*, 102(22):220401, 2009.

[20] Karl-Peter Marzlin and Barry C Sanders. Inconsistency in the application of the adiabatic theorem. *Physical review letters*, 93(16):160408, 2004.

[21] Edward Farhi, Jeffrey Goldstone, Sam Gutmann, Joshua Lapan, Andrew Lundgren, and Daniel Preda. A quantum adiabatic evolution algorithm applied to random instances of an np-complete problem. *Science*, 292(5516):472–475, 2001.

[22] Tameem Albash and Daniel A Lidar. Adiabatic quantum computation. *Reviews of Modern Physics*, 90(1):015002, 2018.

[23] Dorit Aharonov, Wim Van Dam, Julia Kempe, Zeph Landau, Seth Lloyd, and Oded Regev. Adiabatic quantum computation is equivalent to standard quantum computation. *SIAM review*, 50(4):755–787, 2008.

[24] Edward Farhi, Jeffrey Goldstone, and Sam Gutmann. A quantum approximate optimization algorithm. *arXiv preprint arXiv:1411.4028*, 2014.

[25] Leo Zhou, Sheng-Tao Wang, Soonwon Choi, Hannes Pichler, and Mikhail D Lukin. Quantum approximate optimization algorithm: performance, mechanism, and implementation on near-term devices. *arXiv preprint arXiv:1812.01041*, 2018.

[26] David Poulin, Angie Qarry, Rolando Somma, and Frank Verstraete. Quantum simulation of time-dependent hamiltonians and the convenient illusion of hilbert space. *Physical review letters*, 106(17):170501, 2011.

[27] Dong An, Di Fang, and Lin Lin. Time-dependent unbounded hamiltonian simulation with vector norm scaling. *Quantum*, 5:459, 2021.

[28] Guang Hao Low and Nathan Wiebe. Hamiltonian simulation in the interaction picture. *arXiv preprint arXiv:1805.00675*, 2018.

[29] Amir Kalev and Itay Hen. Quantum algorithm for simulating hamiltonian dynamics with an off-diagonal series expansion. *Quantum*, 5:426, 2021.

[30] Rami Barends, Alireza Shabani, Lucas Lamata, Julian Kelly, Antonio Mezzacapo, Urtzi Las Heras, Ryan Babbush, Austin G Fowler, Brooks Campbell, Yu Chen, et al. Digitized adiabatic quantum computing with a superconducting circuit. *Nature*, 534(7606):222–226, 2016.

[31] Sergio Boixo, Emanuel Knill, and Rolando D Somma. Eigenpath traversal by phase randomization. *Quantum Inf. Comput.*, 9(9&10):833–855, 2009.

[32] Kianna Wan and Isaac Kim. Fast digital methods for adiabatic state preparation. *arXiv preprint arXiv:2004.04164*, 2020.

[33] Yimin Ge, András Molnár, and J Ignacio Cirac. Rapid adiabatic preparation of injective projected entangled pair states and gibbs states. *Physical review letters*, 116(8):080503, 2016.

[34] This linear interpolation is not the only possible choice, but we focus on this model throughout the explicit calculations in this work.

[35] Donny Cheung, Peter Høyer, and Nathan Wiebe. Improved error bounds for the adiabatic approximation. *Journal of Physics A: Mathematical and Theoretical*, 44(41):415302, 2011.

[36] Andris Ambainis and Oded Regev. An elementary proof of the quantum adiabatic theorem. *arXiv preprint quant-ph/0411152*, 2004.

[37] Hao-Tien Chiang, Guanglei Xu, and Rolando D Somma. Improved bounds for eigenpath traversal. *Physical Review A*, 89(1):012314, 2014.

[38] Pavel Kos, Marko Ljubotina, and Tomaž Prosen. Many-body quantum chaos: Analytic connection to random matrix theory. *Physical Review X*, 8(2):021062, 2018.

[39] Lin Lin and Yu Tong. Near-optimal ground state preparation. *Quantum*, 4:372, 2020.

[40] Lucas T Brady, Christopher L Baldwin, Aniruddha Bapat, Yaroslav Kharkov, and Alexey V Gorshkov. Optimal protocols in quantum annealing and qaoa problems. *arXiv preprint arXiv:2003.08952*, 2020.

[41] Lucas T Brady, Christopher L Baldwin, Aniruddha Bapat, Yaroslav Kharkov, and Alexey V Gorshkov. Optimal protocols in quantum annealing and quantum approximate optimization algorithm problems. *Physical Review Letters*, 126(7):070505, 2021.

[42] Dong An and Lin Lin. Quantum linear system solver based on time-optimal adiabatic quantum computing and quantum approximate optimization algorithm. *arXiv preprint arXiv:1909.05500*, 2019.

[43] Lucas T Brady, Lucas Kocia, Przemyslaw Bienias, Aniruddha Bapat, Yaroslav Kharkov, and Alexey V Gorshkov. Behavior of analog quantum algorithms. *arXiv preprint arXiv:2107.01218*, 2021.

[44] Jonathan Wurtz and Peter J Love. Counterdiabaticity and the quantum approximate optimization algorithm. *arXiv preprint arXiv:2106.15645*, 2021.

[45] Narendra N Hegade, Koushik Paul, Yongcheng Ding, Mikel Sanz, Francisco Albarrán-Arriagada, Enrique Solano, and Xi Chen. Shortcuts to adiabaticity in digitized adiabatic quantum computing. *Physical Review Applied*, 15(2):024038, 2021.

[46] P Chandarana, NN Hegade, Koushik Paul, F Albarrán-Arriagada, Enrique Solano, A del Campo, and Xi Chen. Digitized-counterdiabatic quantum approximate optimization algorithm. *arXiv preprint arXiv:2107.02789*, 2021.

[47] Friederike Anna Dziemba. Adiabatic quantum computation. *arXiv preprint arXiv:1610.04708*, 2016.

Appendix A: Discrete Riemann-Lebesgue lemma

Lemma 1 (Riemann-Lebesgue lemma). *If $f(x)$ is an L^1 integrable, differentiable function defined on $\mathbb{R}$, $a < b$ are two finite numbers, if $T \gg \max|f(x)|, \max|f'(x)|$, then:*

$$\left| \int_a^b f(x)e^{iTx}dx \right| = \mathcal{O}\left(\frac{1}{T}\right) \tag{A1}$$

Proof. The proof of Riemann-Lebesgue lemma is nothing more than integration by part.

$$\begin{aligned}
\int_a^b f(x)e^{iTx}dx &= \int_a^b f(x)d\left(\frac{e^{iTx}}{iT}\right) \\
&= \left. \frac{f(x)e^{iTx}}{iT} \right|_a^b - \frac{1}{iT}\int_a^b f'(x)e^{iTx}dx
\end{aligned} \tag{A2}$$

$f(x)$ is integrable, thus $f'(x)$ is bounded. Therefore:

$$\left| \int_a^b f(x)e^{iTx}dx \right| \le \frac{1}{T}\left(|f(a)| + |f(b)| + \int_a^b |f'(x)|dx \right) \tag{A3}$$

$\square$

Although the $\mathcal{O}(T^{-1})$ has been proved, the error scaling can actually be improved if $f'(x)$ is also integrable and differentiable. Apply the integration by part again:

$$\int_a^b f(x)e^{iTx}dx = \left.\frac{f(x)e^{iTx}}{iT}\right|_a^b + \frac{1}{T^2}\left[\left. f'(x)e^{iTx}\right|_a^b - \int_a^b f''(x)e^{iTx}dx \right] \tag{A4}$$

$$\left| \int_a^b f(x)e^{iTx}dx \right| \le \frac{1}{T}\left(|f(a)| + |f(b)| \right) + \frac{1}{T^2}\left(|f'(a)| + |f'(b)| + \int_a^b |f''(x)|dx \right) \tag{A5}$$

which is a better upper bound if $T \gg |f'(x)|, |f''(x)|$.

Now we try to extend the results to the discrete version.

Lemma 2. *Given a complex function $z(s) = x(s) + iy(s)$, $s \in [0,1]$, consider the following summation:*

$$\sum_{k=1}^{L} |z_k - z_{k-1}|, \quad z_k := z(s_k), \quad s_k := (k+1)/L \tag{A6}$$

It's upper bounded by:

$$\sum_{k=1}^{L} |z_k - z_{k-1}| \le \int_0^1 |z'(s)|ds \tag{A7}$$

Lemma 3 (Discrete Riemann-Lebesgue lemma (first order)). $f(x)$ *is a L^1 integrable, second-differenable complex function defined on $[0,1]$, $\lambda(x)$ is a positive real function. Denote $f_k := f(s_k)$, then consider the following discrete summation:*

$$J := \frac{1}{L} \sum_{k=1}^{L} f_k \exp[-iT g_k], \quad g_k := \frac{1}{L} \sum_{j<k} \lambda_j \tag{A8}$$

Defining $\delta t := T/L$. If $\delta t \max \lambda(s) < 3.78$ and $T \gg |f/\lambda|$, we have:

$$|J| = \mathcal{O}\left(\max_{s=0,1} \frac{|f(s)|}{T\lambda(s)}\right) + \mathcal{O}\left(\frac{\mathcal{A}(f,\lambda)}{T}\right) \tag{A9}$$

$$\mathcal{A}(f,\lambda) := \int_0^1 |(f(x)/\omega(x))'| \, dx, \quad \omega(x) := (e^{-i\delta t \lambda(x)} - 1)/i\delta t \tag{A10}$$

Proof. Define:

$$\omega_k := \frac{L}{iT}(e^{-iT(g_{k+1}-g_k)} - 1) = \frac{1}{i\delta t}(e^{-i\delta t \lambda_k} - 1) \tag{A11}$$

ω_k is the discrete version of $w(x) = (e^{-i\delta t \lambda(x)} - 1)/i\delta t$, it satisfies:

$$\frac{e^{-iT g_k}}{L} = \frac{e^{-iT g_{k+1}} - e^{-iT g_k}}{iT\omega_k} \tag{A12}$$

Thus, exploit the discrete version of integration by part:

$$\begin{aligned}
J &= \frac{1}{iT} \sum_{k=1}^{L} f_k \frac{e^{-iT g_{k+1}} - e^{-iT g_k}}{\omega_k} \\
&= \frac{1}{iT}\left(\frac{f_L}{\omega_L} e^{-iT g_{L+1}} - \frac{f_0}{\omega_0} e^{-iT g_1} - \sum_{k=1}^{L}\left(\frac{f_k}{\omega_k} - \frac{f_{k-1}}{\omega_{k-1}}\right) e^{-iT g_k}\right)
\end{aligned} \tag{A13}$$

To derive an upper bound for $|J|$, we start with the norm of ω_k:

$$|\omega_k| = \frac{2}{\delta t} \sin\left(\lambda_k \frac{\delta t}{2}\right) \tag{A14}$$

The *sin* function satisfies: $x/2 < \sin(x) < x, \quad x \in (0, 1.89)$. Hence:

$$|\omega_k| = c_k \lambda_k, \quad c_k \in (1,2) \text{ for } \lambda_k \delta t < 3.78 \tag{A15}$$

which implies:

$$\left|\frac{1}{iT}\left(\frac{f_L}{\omega_L} e^{-iT g_{L+1}} - \frac{f_0}{w_0} e^{-iT g_1}\right)\right| < \frac{1}{T}\left(\left|\frac{f_L}{w_L}\right| + \left|\frac{f_0}{w_0}\right|\right) = \mathcal{O}\left(\max_{s=0,1} \frac{|f(x)|}{T\lambda(x)}\right) \tag{A16}$$

Then we focus on the second summation:

$$\left|\frac{-1}{iT} \sum_{k=1}^{L}\left(\frac{f_k}{\omega_k} - \frac{f_{k-1}}{\omega_{k-1}}\right) e^{iT\Lambda_k}\right| \le \frac{1}{T} \sum_{k=1}^{L}\left|\frac{f_k}{\omega_k} - \frac{f_{k-1}}{\omega_{k-1}}\right| \tag{A17}$$

Use Lemma 2, we obtain:

$$\text{RHS} \le \frac{1}{T} \int_0^1 |(f(s)/\omega(s))'| \, ds \tag{A18}$$

$\square$

On the other hand, just like Riemann-Lebesgue lemma, we can apply the "integration by part" step again. The next analysis is the proof of Theorem 1:

Proof. Start with Eq : (A13), we introduce:

$$\eta_k := L \left(\frac{f_k}{\omega_k} - \frac{f_{k-1}}{\omega_{k-1}} \right) \tag{A19}$$

It's the descrete version of:

$$\eta(x) = L \left(\frac{f(s)}{\omega(s)} - \frac{f(s-1/L)}{\omega(s-1/L)} \right) \approx \left(\frac{f(s)}{\omega(s)} \right)' \tag{A20}$$

Then the summation becomes:

$$J := \frac{1}{iT} \left(\frac{f_L}{\omega_L} e^{-iTg_{L+1}} - \frac{f_0}{\omega_0} e^{-iTg_1} - \frac{1}{L} \sum_{k=1}^{L} \eta_k e^{-iTg_k} \right) \tag{A21}$$

Use Lemma 3 on the second part:

$$|J| = \mathcal{O} \left(\max_{s=0,1} \frac{|f(s)|}{T\lambda(s)} \right) + \mathcal{O} \left(\max_{s=0,1} \frac{|\eta(s)|}{T^2\lambda(s)} \right) + \mathcal{O} \left(\frac{\mathcal{A}(\eta, \lambda)}{T^2} \right) \tag{A22}$$

$\square$

Appendix B: Proof of Corollary 1

Proof. The proof largely follows Lemma 4 and Corollary 1 of [35]. The condition Eq. (16), Eq. (17) is used to guarantee that $\Gamma^{(1)}$ is enough to approximate the adiabatic error. In another word, $\epsilon_{\text{adb}} = \mathcal{O}(\sqrt{\sum_{l>0} |\epsilon_l|^2})$. Then we apply Theorem 1 to each of ϵ_l:

$$\epsilon_l = \frac{\theta_l(1)}{iT\omega_l(1)} e^{-i\delta t \sum_{j=0}^{L} \lambda_l(j)} - \frac{\theta_l(0)}{iT\omega_l(0)} e^{-i\delta t \lambda_l(0)} + \mathcal{O} \left(\frac{1}{T^2} \right) \tag{B1}$$

where $\omega_l(x) := (e^{-i\delta t \lambda_l(x)} - 1)/i\delta t$. Lemma 2 tells us that the discrete summation of $|z(s_k) - z(s_{k-1})|$ is trivially bounded by its continuous limit. Thus, the terms generated from "integration by part" can be directly upper bounded by their continuous analogue in [35], except $\{\lambda_l(s)\}$ are replaced with $\{\omega_l(s)\}$. In the region where $|\lambda_l(s)| \leq |\omega_l(s)| \leq 2|\lambda_l(s)|$, we have:

$$|\epsilon_l|^2 = \mathcal{O} \left(\left| \frac{\theta_l(1)}{T\lambda_l(1)} \right|^2 \right) + \mathcal{O} \left(\left| \frac{\theta_l(0)}{T\lambda_l(0)} \right|^2 \right) \tag{B2}$$

Use $\langle l'|0 \rangle + \langle l|0' \rangle = 0$, we further obtain:

$$\sum_{l \neq 0} |\theta_l|^2 = \sum_{l \neq 0} |\langle 0'|l \rangle|^2 \leq \langle 0'|0' \rangle \leq \frac{\|H'\|^2}{\lambda_1^2} \tag{B3}$$

Finally, ϵ_{adb} is upper bounded by:

$$\epsilon_{\text{adb}} = \mathcal{O} \left(\frac{\|H'(1)\|}{T\lambda_1^2(1)} \right) + \mathcal{O} \left(\frac{\|H'(0)\|}{T\lambda_1^2(0)} \right) \tag{B4}$$

$\square$

Appendix C: Adiabatic Theorem with Riemann-Lebesgue Lemma Structure

In this appendix we write one proof of adiabatic theorem with notations of projectors. The method is the same with that of [47]. P is the projector into ground state of non-degenerate Hamiltonian $\bar{H}$ with energy E_0. Defining H as the shifted Hamiltonian such that $H = \bar{H} - E_0 P$, $\quad HP = 0$. $G = \sum_k P_k/(E_k - E_0)$ is the pseudo-inverse of H. It satisfies $GH = HG = I - P$. In previous work [47], it has been proved that:

$$P' = -GH'P - PH'G, \quad G' = PH'G^2 - GH'G + G^2H'P \tag{C1}$$

Consider the following operator:

$$A(s) := \exp_{\mathcal{T}}\left[-iT\int_s^1 H(s)ds\right] \tag{C2}$$

which satifies:

$$A' = iTAH, \quad A'G^2 = iTAG \tag{C3}$$

These are all the elements we need for proving adiabatic theorem. First notice that we are to compare the operator norm between:

$$\epsilon = \|\hat{\epsilon}\| := \|A(1)P(1)A^\dagger(1) - A(0)P(0)A^\dagger(0)\| \tag{C4}$$

It's natural to write $\hat{\epsilon}$ in the form of integral:

$$
\begin{aligned}
\hat{\epsilon} &= \int_0^1 (APA^\dagger)'ds \\
&= \int_0^1 iTAHPA^\dagger + AP'A^\dagger + AP(-iTHA^\dagger)ds \\
&= \int_0^1 AP'A^\dagger ds \\
&= \int_0^1 -AGH'PA^\dagger - APH'GA^\dagger ds
\end{aligned}
\tag{C5}
$$

Two parts are Hermitian conjugate to each other. Use integration by part we can prove every integral like $\int_0^1 AGXPA^\dagger + h.c.ds$ has a factor of $1/T$. From Eq: (C3) we obtain:

$$
\begin{aligned}
\int_0^1 -AGH'PA^\dagger ds &= \frac{i}{T}\int_0^1 A'G^2H'PA^\dagger ds \\
&= \frac{i}{T}\left(AG^2H'PA^\dagger\Big|_0^1 - \int_0^1 A(G^2H'PA^\dagger)'ds\right) \\
&= \frac{i}{T}\left(AG^2H'PA^\dagger\Big|_0^1 - \int_0^1 AGXPA^\dagger ds + \int_0^1 AG^2H'PH'GA^\dagger ds\right)
\end{aligned}
\tag{C6}
$$

with:

$$X = GH'' - 2GH'GH' - H'GH' \tag{C7}$$

This is the stucture of Riemann-Lebesgue lemma. We can apply the integration by part to $\int_0^1 AGXPA^\dagger ds$ again, which results in another factor of T^{-1}. When $T \gg \|X\|, \|X'\|$, it no longer appears in the leading term, thus:

$$
\begin{aligned}
\epsilon &= \left\|\frac{i}{T}\left(AG^2H'PA^\dagger\Big|_0^1 + \int_0^1 AG^2H'PH'GA^\dagger ds\right) + h.c.\right\| + \mathcal{O}\left(\frac{1}{T^2}\right) \\
&= \mathcal{O}\left(\frac{\|H'\|}{T\lambda^2}\right) + \mathcal{O}\left(\frac{\|H'\|^2}{T\lambda^3}\right)
\end{aligned}
\tag{C8}
$$

Of course, there are counterexamples where $\|H''\| = \mathcal{O}(T)$ which make the part including X not negligible.

Corollary 2. *There's no λ^{-3} term in two-level systems.*

Proof. The λ^{-3} terms originates from:

$$\frac{i}{T} \int_0^1 AG[G, H'PH']GA^\dagger ds \tag{C9}$$

In the eigenbasis of $H(s)$, the operators in the commutator have representation:

$$H'|\psi\rangle = \begin{pmatrix} 0 \\ h \end{pmatrix}, \quad H'PH' = \begin{pmatrix} 0 & 0 \\ 0 & |h|^2 \end{pmatrix}, \quad G = \begin{pmatrix} 0 & 0 \\ 0 & \frac{1}{\lambda} \end{pmatrix} \tag{C10}$$

They commute with each other. $\qquad \square$